Quantitative approach to the stochastics of bone remodeling

2012 EPL 97 28009

(http://iopscience.iop.org/0295-5075/97/2/28009)

A Letters Journal Exploring the Frontiers of Physics

January 2012

EPL, **97** (2012) 28009
doi: 10.1209/0295-5075/97/28009

www.epljournal.org

Quantitative approach to the stochastics of bone remodeling

M. Rusconi[1,2(a)], A. Valleriani[2], J. W. C. Dunlop[3], J. Kurths[4,5] and R. Weinkamer[3]

[1] *Center for Dynamics of Complex Systems, Department of Mathematics, University of Potsdam Karl-Liebknecht-Str. 24, 14476 Potsdam, Germany, EU*
[2] *Max Planck Institute of Colloids and Interfaces, Department of Theory and Bio-Systems Science Park Golm, 14424 Potsdam, Germany, EU*
[3] *Max Planck Institute of Colloids and Interfaces, Department of Biomaterials - Science Park Golm, 14424 Potsdam, Germany, EU*
[4] *Humboldt-Universität zu Berlin and Potsdam Institute for Climate Impact Research Telegrafenberg A31, 14473 Potsdam, Germany, EU*
[5] *Institute for Complex Systems and Mathematical Biology, University of Aberdeen Aberdeen AB24 3UE, UK, EU*

received 22 July 2011; accepted in final form 29 November 2011
published online 18 January 2012

PACS 87.85.Tu – Modeling biomedical systems
PACS 02.50.Ga – Markov processes
PACS 87.19.R- – Mechanical and electrical properties of tissues and organs

Abstract – During life bones constantly adapt their structure to their mechanical environment via a mechanically controlled process called bone remodeling. For trabecular bone, this process modifies the thickness of each trabecula leading occasionally to full resorption. We describe the irreversible dynamics of the trabecular thickness distribution (TTD) by means of a Markov chain discrete in space and time. By using thickness data from adult patients, we derive the transition probabilities in the chain. This allows a quantification, in terms of geometrical quantities, of the control of bone remodeling and thus to determine the evolution of the TTD with age.

Introduction. – Architectural changes in trabecular bone, the porous bone found within vertebrae and at the ends of long bones [1], can lead to weakening and fracture of the entire bone organ [2]. In a human vertebra, the trabecular bone consists of a complex network of roughly horizontal and vertical rod and plate-like struts (trabeculae). This trabecular network changes continuously during life due to the regenerative process of bone remodeling. The process of bone remodeling consists in resorption or formation of discrete bone packets by specialized cells [3,4] thus altering the thickness of the trabeculae. Strong local bone resorption may even result in a complete loss of some of the trabeculae, with a preferential loss transverse to the main loading direction in vertebrae leading to an increase in structural anisotropy [5]. This deteriorates the local mechanical stability of the bone thus increasing the risk of spontaneous bone fractures, as seen especially in elderly people [2] and astronauts [6,7]. However, despite the frequent remodeling events the trabecular network is well preserved over the lifetime of a human. This observation suggests that a mechanism controlling remodeling induces an effective protection of thin trabeculae against complete resorption, although not completely avoiding it. In other words, based on this observation we expect that for thin trabeculae the probability of bone formation is larger than the probability of bone resorption. Such a control of bone remodeling can be realized by the action of mechanical forces. Indeed, in the standard mechanostat theory [8] of bone remodeling described by the Wolff-Roux law [9], new bone is locally formed where the local loading is high and removed where the local loading is low. This effectively leads to a protection of thin trabeculae because under the same external force thin trabeculae are more highly strained than thick trabeculae. Although such a mechano-biological law has been successfully implemented in simulations [10–13], the rule remains somewhat qualitative. Even the basic question about the mechanical stimulus that controls bone remodeling is still an open problem. In fact, the quantitative understanding of bone remodeling is hampered by experimental difficulties in

(a) Current address: Bernstein Center for Computational Neuroscience, Charité Universitätsmedizin Berlin - Philippstr. 13, 10115 Berlin, Germany, EU; E-mail: marco.rusconi@bccn-berlin.de

studying the behavior of individual cells in living animals. Nevertheless, recent improvements of 3D-imaging techniques such as magnetic resonance imaging (MRI) and micro-computed tomography (μ-CT) [14] now allow visualizing the complexity of the trabecular architecture even in living small animals. These techniques, while delivering snapshots of the architectural structure of the bone in terms of geometrical quantities, provide little insight into the dynamics of the processes of bone remodeling. It is thus the aim of theory and models to fill this gap and suggest mechanisms that are compatible with the results from these imaging techniques.

In this work we extract quantitative information about the control of bone remodeling, by applying classical tools from mathematical physics to 3D tomographic data sets. In our approach, the control of bone remodeling is expressed in terms of trabecular architecture and not in terms of mechanical loading. The advantage of this approach is that we can directly build on the experimental data provided by μ-CT and we do not need any assumptions about the nature of the mechanical stimulus. Our main result is expressed in the form of two remodeling rules (RRs) that give the probability of local bone resorption or deposition as a function of the local trabecular thickness. These RRs can then be used to predict structural changes with age, such as the increase of anisotropy, observed in the trabecular structure. In a second step, we use an assumption about the loading of trabeculae in order to interpret our results in the context of a mechano-biological control of bone remodeling.

The model. – In our model, the trabecular network within a vertebra is considered as a collection of individual trabeculae, each characterized by its cross-sectional area A. We describe the trabecular architecture by the trabecular area distribution (TAD), which gives the probability of finding a trabecula with cross-sectional area A. Due to bone remodeling, the cross-sectional area of each trabecula evolves with time, and, therefore, the TAD is also a time dependent quantity. In a single remodeling event, a bone packet is resorbed or deposited at the surface of the trabecula. A remodeling event can be viewed as either increasing or decreasing A by a discrete amount ΔA. By discretizing area in units of ΔA, each trabecula in the vertebra can be considered to be in a state i with cross-sectional area $A_i = i\Delta A$, $i = 0, 1, \ldots, N_{\max}$. Bone remodeling can then be described as a one-dimensional stochastic process whose state space is the set of discrete values A_i of the cross-sectional area. With p_i we denote the probability per unit time that at a given trabecula a bone packet is deposited, *i.e.* that A_i changes to state $A_{i+1} = A_i + \Delta A$; q_i denotes the probability of a resorption event, *i.e.* that A_i changes to state $A_{i-1} = A_i - \Delta A$. If the time step Δt is chosen to be small enough, then only one single remodeling event will occur in a single trabecula during this time. Therefore, there is a zero probability of increasing or decreasing the cross-sectional area by more than ΔA. The probability r_i that no deposition or resorption occurs and that the trabecula remains in its current state is $r_i = 1 - q_i - p_i$. As new bone can only be formed on the surface [3,4], a completely resorbed trabecula, *i.e.* in the state $i = 0$, cannot be reformed. The state $i = 0$ is therefore an *absorbing state* of the Markov chain. This implies that the time evolution of the TAD is irreversible. For $i = N_{\max}$ reflecting boundary conditions were applied. Under our assumptions, bone remodeling is naturally described as a one-dimensional absorbing random walk, discrete in time and space, in which the "walker's" position is the trabecular cross-sectional area and transitions are possible only between nearest neighbors. The time evolution of the process is thus described by a tridiagonal *transition matrix* $\mathbb{P}$ whose upper, main and lower diagonals are, p_i, r_i and q_i, respectively:

$$\mathbb{P} = \begin{pmatrix} 1 & 0 & 0 & 0 & 0 \\ q_1 & r_1 & p_1 & 0 & 0 \\ 0 & q_2 & r_2 & p_2 & 0 \\ \vdots & & & \ddots & \vdots \\ 0 & \ldots & \ldots & q_{N_{\max}} & 1 - q_{N_{\max}} \end{pmatrix}.$$

Model parameters. The basic model parameters are chosen based on experimental data of trabecular bone remodeling. The mean thickness of a trabecula, D is about $170\,\mu$m. During a single remodeling event in trabecular bone, a roughly longitudinal, semi-cylindrical "trench" [15–18] is remodeled along the trabecula. The bone packet produced by this event, we approximate as a half-cylinder with a depth of $40\,\mu$m [16], corresponding to a $\Delta A \approx 2500\,\mu\text{m}^2$. Assuming a circular cross-section for the whole trabecula [19], 10 remodeling events are therefore necessary to remodel its equivalent volume. This so-called turnover time to remodel the whole bone volume is around 5 years for trabecular bone [20]. We chose a time step Δt of 3 days, which is short enough to prevent multiple remodeling events, and $N_{\max} = 50$, which is large enough to avoid artifacts from the reflecting boundary conditions. Since on average in 5 years 10 remodeling events take place, the mean probability of a remodeling event sigma within the time step $\Delta t = 3$ days can be estimated as

$$\sigma = 10\frac{3\text{ days}}{5\text{ years}} \approx 0.016.$$

The aging of the trabecular thickness distribution. Although a formulation of our model in terms of cross-sectional area is natural, since then the different states are equidistant in area, the scientific community working in the bone field prefers the thickness to characterize the trabecular structure [5]. From the assumption of cylindrical trabeculae, the transformation from states in area into states in thickness is straightforward:

$$T_i = \sqrt{\frac{4i\Delta A}{\pi}},$$

with $i = 0, \ldots, N_{\max}$. The outcome of a 3D imaging experiment, and also the quantity characterizing the trabecular architecture in the model is then the trabecular thickness distribution, **TTD**. TTD_i defines the probability to find a trabecula with a thickness within the range of T_i and $T_{i+1} = T_i + \Delta T_i$. Once the transition matrix $\mathbb{P}$ and an initial distribution **TTD**(0) is given, the **TTD** after the time $\tau \Delta t$ can be easily computed as

$$\mathbf{TTD}(\tau) = \mathbf{TTD}(\mathbf{0})\mathbb{P}^{\tau}. \tag{1}$$

In the following we exploit our model approach and eq. (1) in two directions. First, assuming a steady-state situation at the end of adolescence we demonstrate that an experimentally measured **TTD** can be used to extract information about the transition matrix, *i.e.* information of how remodeling is controlled. In a second step the obtained RRs are used to investigate how the trabecular architecture evolves with time due to continuous remodeling. Our predictions are then compared with recently reported experimental data [5].

Steady state. In contrast to adult bone, during childhood and adolescence bone remodeling occurs concurrently with growth. We describe this in the model by adding new trabeculae during growth with thicknesses close to the mean thickness D. At the end of adolescence, when the growth slows down, the rate of newly formed and resorbed trabeculae should be equal and rather small [21]. Therefore, we assume that at around this time the **TTD** is in a steady state. Denoting $\mathbf{\Pi}$ this stationary distribution, it therefore fulfills the condition

$$\mathbf{\Pi} = \mathbf{\Pi}\tilde{\mathbb{P}}.$$

The only difference in the transition matrices $\mathbb{P}$ and $\tilde{\mathbb{P}}$ is that the state $i = 0$ is not an absorbing state, *i.e.* $\mathbb{P}_{00} = 1$. This is because during growth new trabeculae are assumed to form at the same rate as they are resorbed. We also assume that all the newly formed trabeculae have the same mean thickness D, therefore, $\tilde{\mathbb{P}}_{0\tilde{N}} = 1$ with

$$\tilde{N} \approx \frac{1}{4}\frac{\pi D^2}{\Delta A}.$$

The remodeling process at this phase when the growth of the vertebra comes to an end is thus described as a repeated Markov process [22] with $\tilde{N}$ denoting the returning point. In the following we will show how, based on a measured $\mathbf{\Pi}$, the steady-state conditions can be used to extract the RRs.

Materials. – A high-resolution μ-CT scan of the whole lumbar vertebra of a healthy man with a resolution of $37\,\mu$m [23] was used to obtain $\mathbf{\Pi}$ with the ball fitting method [24]. Figure 1 shows the experimental probability density function $\pi^{\exp}$, $\sum \pi_i^{\exp} \Delta T^{\exp} = 1$, where $\Delta T^{\exp}$ was twice the experimental resolution.

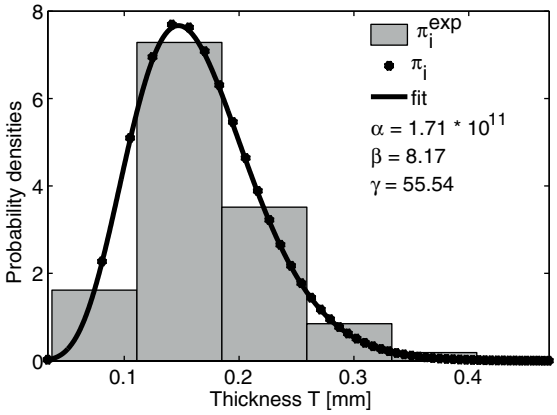

Fig. 1: Experimentally obtained probability density function of the thickness of trabeculae within a human lumbar vertebra. The data was fitted by $F(T) = \alpha T^{\beta} \exp(-\gamma T)$ with α, β and γ being fit parameters when T is measured in mm. The datapoints π_i marked as points on the fitting curve were used as input for eqs. (2) to calculate the remodeling rules.

Resampling of the experimental distribution. Due to the limited resolution of today's μ-CT of large samples, we resampled the data in units of ΔA. The asymmetric experimental distribution (see fig. 1) was fitted with a Planck-like function,

$$F(T) = \alpha T^{\beta} \exp(-\gamma T),$$

where α, β, γ are the fitting parameters. The fitting function is now evaluated at the mid-points

$$\bar{T}_i = \sqrt{\frac{\Delta A}{\pi}}(\sqrt{i} + \sqrt{i-1})$$

and $\bar{T}_0 = 0$, to get the re-sampled experimental probability density, $\pi_i = F(\bar{T}_i)$ (fig. 1). The normalization requires

$$\sum_{i=0}^{N_{\max}} F(\bar{T}_i)\Delta T_i = 1.$$

Results and discussion. –

The remodeling rules from the data. Using the experimental π_i, the steady-state condition reads

$$\pi_i \Delta T_i = \sum_{j=0}^{N_{\max}} \pi_j \Delta T_j \tilde{\mathbb{P}}_{ji},$$

where $i = 1, \ldots, N_{\max}$. Of this system of $N_{\max}$ linear algebraic equations, only $N_{\max} - 1$ are independent due to the normalization condition. The system is clearly underdetermined, since it includes the $2N_{\max} - 1$ unknown p_i and q_i of the RRs. We investigate the special cases that one RR is constant. When bone remodeling is controlled only via bone deposition [11,12], *i.e.* $q_i = \sigma$, then the solution of the system for p_i gives

$$\begin{aligned} p_i &= \sigma \frac{\pi_{i+1} - \pi_1}{\pi_i}, \quad i = 1, \ldots, \tilde{N} - 1, \\ p_i &= \sigma \frac{\pi_{i+1}}{\pi_i}, \qquad\quad i = \tilde{N}, \ldots, N_{\max} - 1. \end{aligned} \tag{2}$$

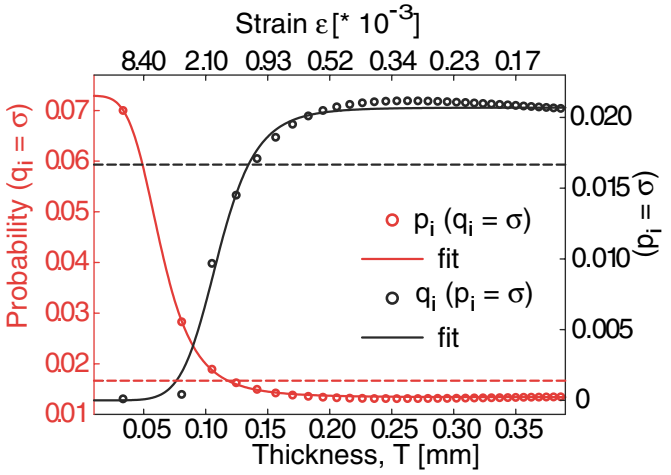

Fig. 2: (Color online) Remodeling rules for bone deposition assuming a constant probability for bone resorption, $q_i = \sigma$ (red) using eqs. (2), and for bone resorption assuming a constant probability for bone deposition, $p_i = \sigma$ (black).

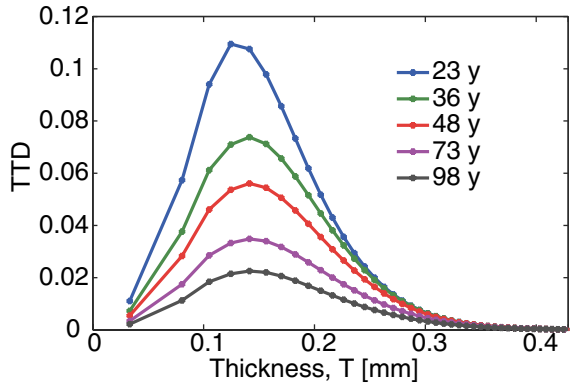

Fig. 3: (Color online) Trabecular thickness distribution, **TTD**, as a function of age (colors). The initial **TTD** was obtained multiplying by ΔT_i the experimental distribution from fig. 1 corresponding to a healthy individual. With time, the probability is accumulated into the absorbing state (not shown).

Analogous results are obtained when bone remodeling is controlled via resorption, *i.e.* $p_i = \sigma$.

The RR controlling bone deposition from eqs. (2) is plotted in fig. 2, red frame of the inset, for $\sigma = 0.016$. The deposition probability p_i has large values for small trabecular thickness, it decreases then abruptly and takes almost constant values (slightly below the constant resorption probability, dashed red line) for large values of the thickness. Such a remodeling rule protects thin trabeculae from complete resorption. A similar behavior, but with opposite sign, is obtained when deposition is assumed to be independent of thickness ($p_i = \sigma$, black dashed line), and remodeling is controlled via resorption (fig. 2, black frame). The resorption probability takes small values for thin trabeculae, and is described by a sigmoidal curve, increasing with thickness. The data of fig. 2 for both p_i and q_i were fitted by a Hill function:

$$R(T) = y_0 + \frac{aT^b}{c^b + T^b}, \tag{3}$$

where y_0, a, b, and c are fitting parameters. The exponent b governs the steepness of the control function, while the activation coefficient c describes at which thickness the control is significantly activated. The corresponding fit values for constant resorption ($q_i = \sigma$) are $y_0 = 0.013$, $a = 0.059$, $b = -4.63$, $c = 0.064\,\mathrm{mm}$; and for constant deposition ($p_i = \sigma$) $y_0 = 0$, $a = 0.02$, $b = 7.16$, $c = 0.11\,\mathrm{mm}$. The high values for b are in good agreement with a recent finding suggesting that the control of bone remodeling may be reasonably described with a step function, *i.e.* a threshold value controls the activation/deactivation of bone deposition [12].

Mechano-biological interpretation of the remodeling rules. Our method allows the quantification of the Wolff-Roux law controlling bone remodeling in terms of a measurable geometrical quantity, the trabecular thickness. There is common agreement that this control in bone occurs via mechanical stimulation of cells, which transmit this information to the bone surface, where bone resorption and deposition occurs [3,4]. With simple mechanical considerations, we can interpret the resulting RRs along these lines. Assuming that each rod-like trabecula is loaded with a roughly equal force along its long axis, the strain ϵ will be proportional to the cross-sectional area, *i.e.* $\epsilon = K/T^2$, where

$$K = \frac{4}{\pi E}\frac{F}{A_V(\mathrm{Tb.N})^2} \tag{4}$$

and $A_V = 1200\,\mathrm{mm}^2$ is the vertebra cross-section. For the trabeculae within a vertebra, K can be estimated by the applied stress on the vertebral core of trabecular bone (due to a force $F = 500\,\mathrm{N}$, [25,26]), the number of trabeculae per length unit ($1.3\,\mathrm{mm}^{-1}$), and the stiffness of the bone material ($E = 15\,\mathrm{GPa}$) with the result $K \sim 2.1 \cdot 10^{-5}\,\mathrm{mm}^2$. The inverse quadratic relation between ϵ and T reduces the Hill exponent when plotting the RR over the strain (fig. 2, x-axis on top) by a factor of 2.

Aging of the trabecular structure. The knowledge of the RRs and an initial experimental TTD can be used to calculate, by means of eq. (1), the aging of the trabecular architecture characterized by its TTD. $\mathbf{TTD}(0) = \mathbf{\Pi}$ was used as an initial condition with the RRs, where resorption is thickness independent ($q_i = \sigma$) [11,12]. Figure 3 shows how the **TTD** evolves with time starting from an age of about 23 years (blue line). Due to the loss of trabeculae by complete resorption during remodeling, the peak height of the distribution decreases, while the absorbing state of zero thickness (not shown) becomes more populated. The peak of the distribution shifts slightly towards larger values of the thickness, while the asymmetric shape of the distribution is largely conserved.

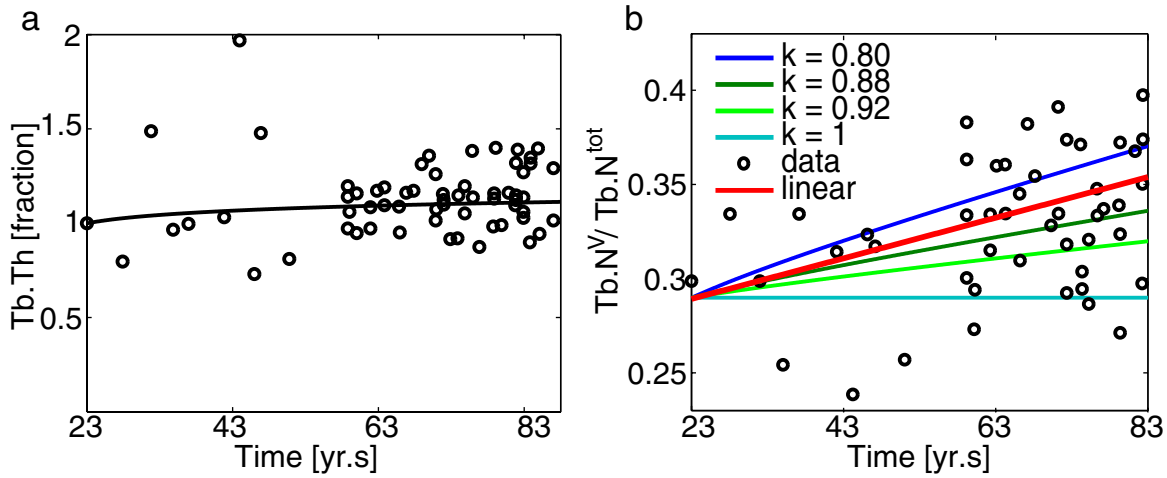

Fig. 4: (Color online) (a) Time evolution of the fraction of trabecular thickness, comparison between computational results (solid) and experiments (circles) [5]. The quantities are normalized to 1 at the first available datapoint from a patient of 23 years of age (the first datapoint of [5]). (b) Time evolution of the proportion of vertical trabeculae, $\mathrm{Tb.N^V/Tb.N^{tot}}$, for different reductions of the horizontal load. The parameter k denotes how much of the vertical load is applied in horizontal direction. Simulation results are compared with experimental data from [5] and with a linear fit of the data (red line, $y = 0.0011\,x + 0.29$).

The structural changes of the trabecular architecture with age are usually reported by averaged quantities [27], such as: the bone volume fraction (BV/TV), the mean trabecular thickness (Tb.Th), and the trabecular number, Tb.N. All these quantities can be easily calculated from the **TTD**. The Tb.Th is given by the $\mathrm{Tb.Th}(\tau) = \sum_{i=0}^{N_{\max}} T_i\, TTD_i(\tau)$, and the normalized trabecular number is calculated as $\mathrm{Tb.N}(\tau) = \sum_{i=1}^{N_{\max}} TTD_i(\tau)$. The continuous line in the inset of fig. 4(a) shows the fraction of Tb.Th, normalized to 1 for the young adult (23 years in the plot). While the bone volume decreases with age due to the loss of trabeculae, the Tb.Th increases monotonically. For an age of 83 years, Tb.Th has increased about 8%. The architectural changes of trabecular bone with the loss of trabeculae and the increase of thickness of the remaining ones can be summarily described as a process of coarsening [13]. The circles in fig. 4(a) refer to experimental data of Tb.Th fraction of vertebrae of different age (data from fig. 2(F) in [5]). The calculated rate of trabecular thickening agrees well with the experimental measurements. The large experimental scatter arises as these kind of *postmortem* investigations can be performed in humans only in a cross-sectional study, *i.e.* taking vertebrae of different individuals with different ages.

Another structural change of trabecular bone with age is the increase in anisotropy due to a preferential loss of horizontal trabeculae. We assume that horizontal trabeculae experience a lower load than vertical ones [13], $F' = Fk$ with $k \in [0, 1]$. We assume that the mechanosensitivity of the bone is unchanged, *i.e.* the remodeling rule expressed in a mechanical quantity like the strain ϵ is unchanged, $R'(\epsilon) = R(\epsilon)$. Using (see above eq. (4)) $\epsilon = K/T^2 = kK/T'^2$ and making the following variable transformations, $R(T) \to R(\epsilon) = R'(\epsilon) \to R'(T')$, gives the result that $R'(T')$ has the same functional form like $R(T)$, only the coefficient c changes to $c' = \sqrt{k}\, c$. With this unequal loading in vertical and horizontal direction our model can predict the time development of anisotropy. To allow a comparison with experimental results from [5], we evaluated the proportion of vertical trabeculae, $\mathrm{Tb.N^V/Tb.N^{tot}}$, as a function of age. The better conservation of vertical compared to horizontal trabeculae results in a roughly linear increase of $\mathrm{Tb.N^V/Tb.N^{tot}}$ (fig. 4(b)). The slope is larger for a stronger decrease of the load in horizontal direction. Using different values of k to predict the time evolution of the structural anisotropy, good agreement with the experimental data is obtained when the horizontal load is about 85% of the vertical load (fig. 4(b)).

Conclusion. – In this letter the architectural changes due to bone remodeling have been described as a one-dimensional random walk whose state space is defined by the discrete value set of the trabecular cross-sectional area (thickness).

In computational studies of bone remodeling usually a phenomenological remodeling rule is assumed and the trabecular architecture resulting from this RR is then obtained in the computer simulation. The clear drawback of this approach is that the mathematical form of the remodeling rule is introduced without justification, *a priori*. In this letter we introduce a method that results in an "inversion of the problem". The RRs, *i.e.* the control of bone remodeling, have been inferred from experimental data of the local trabecular structure. This inverse problem is much more complicated and requires model assumptions concerning bone remodeling and the trabecular architecture. A great benefit of these assumptions is to be able to obtain the RRs shown in fig. 2.

Our approach leads to the quantification of the control of bone remodeling in terms of trabecular geometry. Using mechanical considerations this result can be interpreted in terms of the standard mechanobiological Wolff-Roux law.

In the final part of this letter, having obtained the RRs, we predicted the aging of the trabecular structure inside a human vertebra. The aging was quantified by computing the time course of the trabecular thickness distribution describing the population of trabeculae in the structure. To compare our prediction with the only currently available experimental data, we computed the standard averaged quantity describing the bone loss, the coarsening of the structure, and the increase in structural anisotropy. Our results are in good agreement with the experimental evidence.

To develop computational tools to conclude from the observed macroscopic architecture on the microscopic behavior of cells, which carry out the remodeling of bone, is an urgent problem. Recent progress in imaging techniques allows that architectural changes in bone can be followed *in vivo* [28] and in addition improved medications allow specific targeting of bone resorption and deposition [29]. Computational tools allowing microscopic (time-dependent) cell behaviors to be interpreted from static macroscopic images, can circumvent the inherent difficulties of *in vivo* cell experiments and greatly enhance the amount of information that can be extracted from 3D imaging. The large interpersonal variations make it necessary to use model approaches as presented here to perform a patient-specific interpretation of the trabecular architecture in terms of the underlying control and to predict architectural changes with age.

* * *

MR was supported by the Marie Curie "Early Stage Training on Biomimetic Systems".

REFERENCES

[1] Cowin S. C. and Doty S. B., *Tissue Mechanics* (Springer) 2007; Currey J. D., *Bones* (Princeton University Press) 2002.
[2] Seeman E. and Delmas P. D., *N. Engl. J. Med.*, **354** (2006) 2250.
[3] Fratzl P. and Weinkamer R., *Prog. Mater. Sci.*, **52** (2007) 1263.
[4] Robling A. G., Castillo A. B. and Turner C. H., *Annu. Rev. Biomed. Eng.*, **7** (2006) 455.
[5] Stauber M. and Müller R., *Osteoporos. Int.*, **17** (2006) 616.
[6] Morey E. R. and Baylink D. J., *Science*, **201** (1978) 1138.
[7] Rusconi M., Zaikin A., Marwan N. and Kurths J., *Phys. Rev. Lett.*, **100** (2008) 128101.
[8] Frost H. M., *Anat. Rec.*, **219** (1987) 1.
[9] Wolff J., *Das Gesetz der Transformation der Knochen* (Hirschwald, Berlin) 1892; Roux W., *Arch. Anat. Physiol. Anat. Abt.* (1885) 120.
[10] Thomsen J. S. *et al.*, *Bone*, **15** (1994) 655.
[11] Huiskes R., Ruimerman R., van Lenthe G. H. and Janssen J. D., *Nature*, **405** (2000) 704.
[12] Dunlop J. W. C. *et al.*, *Calcif. Tissue Int.*, **85** (2009) 45.
[13] Weinkamer R., Hartmann M. A., Brechet Y. and Fratzl P., *Phys. Rev. Lett.*, **93** (2004) 228102.
[14] Muller R., *Nat. Rev. Rheumatol.*, **5** (2009) 373.
[15] Parfitt A. M., *J. Cell. Biochem.*, **55** (1994) 273.
[16] Jee W. S. S., in *Bone Mechanics Handbook*, edited by Cowin S. C. (CRC Press) 2001.
[17] Morgan E. F., Barnes G. L. and Einhorn T. A., in *Fundamentals of Osteoporosis*, edited by Marcus R. (Academic Press) 2010, Chapt. 1.
[18] Fleisch H., *Bisphosphonates in Bone Disease: From the Laboratory to the Patient* (Academic Press) 2000.
[19] van Lenthe G. H., Stauber M. and Müller R., *Bone*, **39** (2006) 1182.
[20] Eriksen E. F., Melsen F., Sod E., Barton I. and Chines A., *Bone*, **31** (2002) 620.
[21] Seeman E., *J. Bone Miner. Metab.*, **26** (2008) 1.
[22] Hill T. L., *Proc. Natl. Acad. Sci. U.S.A.*, **85** (1988) 4577.
[23] Bone 3D Project Team (ESA MAP Project AO-99-030 ESTEC Contract #14592/00/NL/SH).
[24] Hildebrand T. and Rüegsegger P., *J. Microsc.*, **185** (1997) 67.
[25] Adams M. A. and Dolan P., *Clin. Biomech.*, **10** (1995) 3.
[26] Homminga J. *et al.*, *Bone*, **34** (2004) 510.
[27] Parfitt A. M. *et al.*, *J. Bone Miner. Res.*, **2** (1987) 595.
[28] Schulte F. A., Lambers F. M., Kuhn G. and Müller R., *Bone*, **48** (2011) 433.
[29] Delmas P. D., *Lancet*, **359** (2001) 2018.